

Crumpling transition of the discrete planar folding in the negative-bending-rigidity regime

Yoshihiro Nishiyama (西山由弘)

Department of Physics, Faculty of Science, Okayama University, Okayama 700-8530, Japan

(Received 28 March 2010; published 23 July 2010)

The folding of the triangular lattice embedded in two dimensions (discrete planar folding) is investigated numerically. As the bending rigidity K varies, the planar folding exhibits a series of crumpling transitions at $K \approx -0.3$ and $K \approx 0.1$. By means of the transfer-matrix method for the system sizes $L \leq 14$, we analyze the singularity of the transition at $K \approx -0.3$. As a result, we estimate the transition point and the latent heat as $K = -0.270(2)$ and $Q = 0.043(10)$, respectively. This result suggests that the singularity belongs to a weak-first-order transition.

DOI: [10.1103/PhysRevE.82.012102](https://doi.org/10.1103/PhysRevE.82.012102)

PACS number(s): 05.50.+q, 82.45.Mp, 05.10.-a, 46.70.Hg

At sufficiently low temperatures, a polymerized membrane becomes flattened macroscopically [1]; see Refs. [2–5] for a review. It still remains unclear [6–8] whether the crumpling transition (separating the flat and crumpled phases) is critical [9–21] or belongs to a discontinuous one with an appreciable latent heat [22–24].

In this Brief Report, we investigate a discretized version of the polymerized membrane embedded in two dimensions [25–28]; details are overviewed afterward. This model, the so-called discrete planar folding, exhibits a series of crumpling transitions at $K \approx -0.3$ and 0.1 [27,28], as the bending rigidity K changes. The latter transition exhibits a pronounced discontinuous character, whereas the nature of the former transition remains unclear. In this Brief Report, we utilized the transfer-matrix method [27] for the system sizes $L \leq 14$. We implemented a modified folding rule [29] [Eq. (5)], which enables us to impose the periodic-boundary condition. Technically, the restoration of the translational symmetry admits a substantial reduction in the transfer-matrix size.

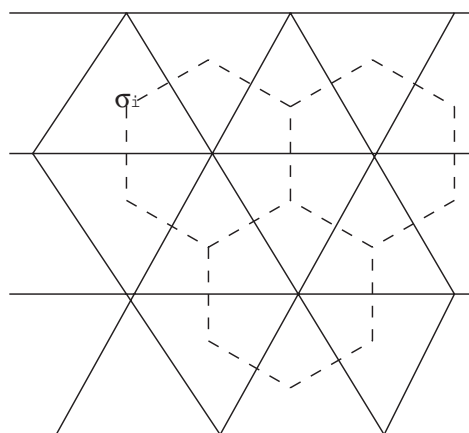
To begin with, we explain a basic feature of the discrete planar folding [27,28]; see Fig. 1(a). We consider a sheet of the triangular lattice. Along the edges, the sheet folds up. The fold angle θ is either $\theta=0$ (complete fold) or π (no fold). The elastic energy at each edge is given by $K \cos \theta$ with the bending rigidity K . The thermodynamic property of the planar folding has been studied extensively [27,28]. The transfer-matrix simulation for the system sizes $L \leq 9$ [27] revealed a series of crumpling transitions at $K \approx -0.3$ and $K=0.11(1)$. The behavior of the specific heat around $K \approx -0.3$ indicates that this transition would be a continuous one. The cluster variation method (CVM) of a single-hexagon-cluster approximation [28] indicates that there occur crumpling transitions at $K=-0.284$ and $K=0.1013$ of the continuous and discontinuous characters, respectively.

The crumpling transition $K \approx -0.3$ is closely related [32] to that of an extended folding [30–32] at $K_3 \approx -0.8$. (The extended folding, the so-called three-dimensional folding, has four possibilities, $\cos \theta = \pm 1, \pm 1/3$, as to the joint angle θ .) That is, according to an argument based on a truncation of the configuration space [32], the following (approximate) relations should hold:

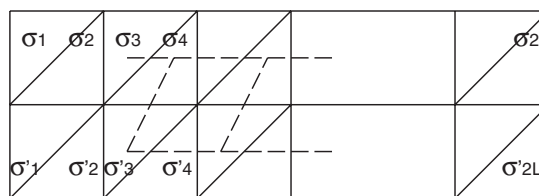
$$K = K_3/3, \quad (1)$$

$$Q = Q_3. \quad (2)$$

Here, the variables Q and Q_3 denote the latent heat for the planar- and three-dimensional-folding models, respectively. A number of results, $(K_3, Q_3) = (-0.852, 0)$ [32], $(-0.76(1), 0.03(2))$ [33], and $(-0.76(10), 0.05(5))$ [29], have been obtained via the CVM, density-matrix renormalization-group, and exact-diagonalization analyses, respectively. The nature of its transition at $K_3 \approx -0.8$ is not fully clarified, because the three-dimensional folding is computationally demanding. It is a purpose of this Brief Report to shed light on



(a)



(b)

FIG. 1. (a) We consider a discrete folding of the triangular lattice. The fold angle (with respect to the adjacent triangular plaquettes) is discretized into either $\theta=0$ or π . (b) A drawing of a transfer-matrix strip is shown.

this longstanding issue from the viewpoint of the planar folding. (It has to be mentioned that the planar folding has relevance to a wide class of systems [26,34–37].)

For the sake of self-consistency, we present the transfer-matrix formalism for the discrete planar folding explicitly. We place the Ising variables $\{\sigma_i\}$ at each triangle i (rather than each joint); see Fig. 1(a). Hereafter, we consider the spin model on the dual (hexagonal) lattice. The Ising-spin configuration specifies each joint angle between the adjacent triangles. That is, provided that the spins are (anti)parallel, $\sigma_i\sigma_j=1$ (-1), for a pair of adjacent neighbors, i and j , the joint angle is $\theta=\pi$ (0). The spin configuration is subjected to a constraint (folding rule); the prefactor of the transfer-matrix element [Eq. (3)] enforces the constraint. As a consequence, the discrete folding reduces to an Ising model on the hexagonal lattice. In Fig. 1(b), a drawing of the transfer-matrix strip is presented. The row-to-row statistical weight $T_{\{\sigma_i\},\{\sigma'_i\}}$ yields the transfer-matrix element. The transfer-matrix element for the strip length L is given by [27]

$$T_{\{\sigma'_i\},\{\sigma_i\}} = \left(\prod_{i=1}^L \delta(\sigma_{2i} + \sigma_{2i+1} + \sigma_{2i+2} + \sigma'_{2i-1} + \sigma'_{2i} + \sigma'_{2i+1} \bmod 3, 0) \right) \exp\left(-\sum_{i=1}^L H_i(K)/T\right), \quad (3)$$

with the local Hamiltonian

$$H_i(k) = -\frac{K}{2}(\sigma_{2i}\sigma_{2i+1} + \sigma_{2i+1}\sigma_{2i+2} + \sigma_{2i+2}\sigma'_{2i+1} + \sigma'_{2i+1}\sigma'_{2i} + \sigma'_{2i}\sigma'_{2i-1} + \sigma'_{2i-1}\sigma_{2i}), \quad (4)$$

due to the bending-energy cost for spins surrounding each hexagon i . Here, the parameter K denotes the bending rigidity, and the expression $\delta(n, m)$ is Kronecker's symbol. The periodic-boundary condition $\sigma_{L+i}=\sigma_i$ is imposed. We set $T=1$, considering it as a unit of energy.

In practice, the above scheme does not work. The folding rule is too restrictive to impose the periodic-boundary condition. So far, the open-boundary condition has been implemented; more specifically, the range of the running index i in Eq. (3) was set to $1 \leq i \leq L-1$ [27]. In this Brief Report, following Ref. [29], we make a modification as to the constraint [prefactor of Eq. (3)] to surmount the difficulty. We replace the above expression with

$$T_{\{\sigma'_i\},\{\sigma_i\}} = \frac{1}{L} \sum_{l=1}^L \left(\prod_{i \neq l} \delta(\sigma_{2i} + \sigma_{2i+1} + \sigma_{2i+2} + \sigma'_{2i-1} + \sigma'_{2i} + \sigma'_{2i+1} \bmod 3, 0) \right) \exp\left(-\sum_{i \neq l} H_i(K) - H_l(K')\right). \quad (5)$$

That is, the constraint is released at a defect hexagon $i=l$. Additionally, the local bending rigidity at the defect is set to K' . In order to improve the finite-size behavior, we adjust K' to

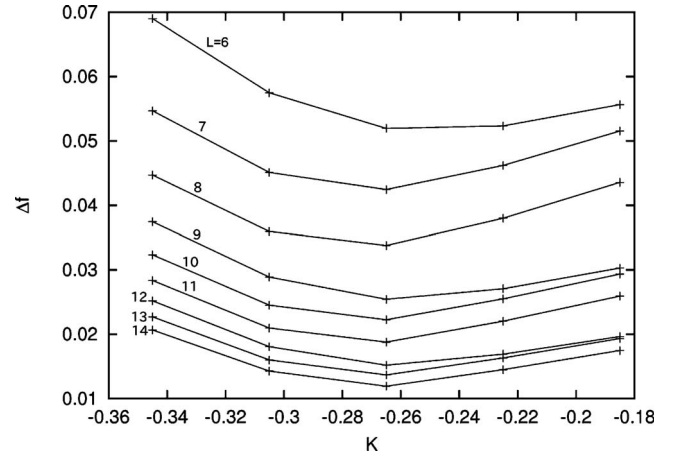


FIG. 2. The free-energy gap (7) is plotted for the bending rigidity K and the system sizes $6 \leq L \leq 14$.

$$K' = 2K. \quad (6)$$

A justification is shown afterward.

Based on the transfer-matrix formalism with a modified folding rule (5), we simulated the planar folding numerically. The numerical diagonalization was performed within a subspace specified by the wave number $k=0$ and the parity even; here, we made use of the spin-inversion symmetry $\sigma_i \rightarrow -\sigma_i$.

In Fig. 2, we plot the free-energy gap

$$\Delta f = f_2 - f_1, \quad (7)$$

for the bending rigidity K and various system sizes $L=6, 7, \dots, 14$. Here, the free energy per unit cell is given by $f_i = -\ln \Lambda_i / (2L)$ with the (sub)dominant eigenvalue $\Lambda_{1(2)}$ of the transfer matrix. (Here, the unit cell stands for a triangle of the original lattice rather than a hexagon of the dual lattice; see Fig. 1.) From Fig. 2, we see a signature of a crumpling transition (closure of Δf) at $K \approx -0.27$. The location of the transition point appears to be consistent with the preceding estimates [27,28].

In Fig. 3, the approximate transition point $K(L)$ is plotted for $1/L^2$ and $6 \leq L \leq 14$. The approximate transition point minimizes Δf ; namely, the relation

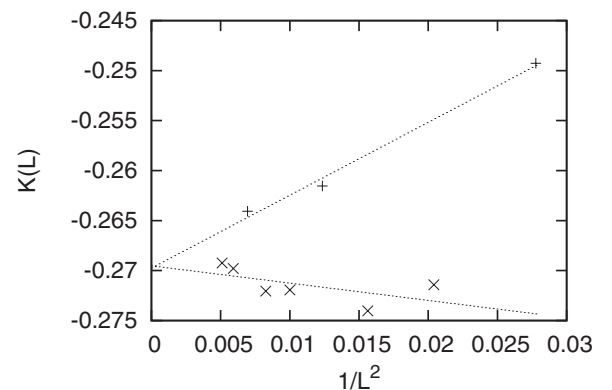


FIG. 3. The transition point $K(L)$ (8) is plotted for $1/L^2$. The linear least-squares fit for $L=0$ (+) and $1, 2 \bmod 3$ (x) ($6 \leq L \leq 14$) yields $K = -0.2697(12)$ and $-0.2695(14)$, respectively.

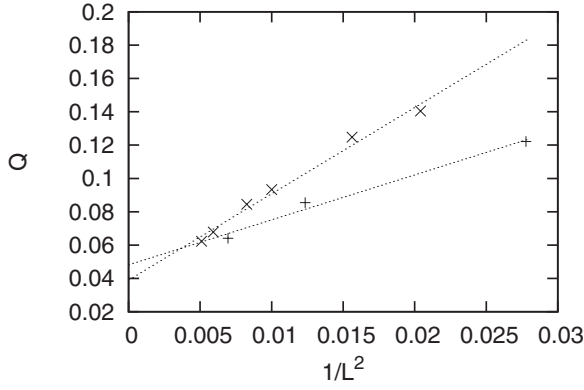


FIG. 4. The latent heat $Q(L)$ (11) is plotted for $1/L^2$. The linear least-squares fit for $L=0$ (+) and $1, 2 \bmod 3$ (\times) ($6 \leq L \leq 14$) yields $Q=0.0482(59)$ and $0.0391(38)$, respectively.

$$\partial_K \Delta f|_{K=K(L)} = 0 \quad (8)$$

holds. The least-squares fit to a series of results for $L=6, 9, 12$ yields an estimate $K=-0.2697(12)$ in the thermodynamic limit $L \rightarrow \infty$. Similarly, for $L=1, 2 \bmod 3$, we obtain $K=-0.2695(14)$. (An observation that the data $L=0$ and $1, 2 \bmod 3$ behave differently was noted in Ref. [27].) The above independent results appear to be consistent with each other, validating the $1/L^2$ -extrapolation scheme. As a result, we estimate the transition point as

$$K = -0.270(2). \quad (9)$$

We then proceed to estimate the amount of the latent heat with Hamer's method [38]. A basis of this method is as follows. At the first-order transition point, the low-lying spectrum of the transfer matrix exhibits a level crossing, and the discontinuity (sudden drop) of the slope reflects a release of the latent heat. However, the finite-size artifact (level repulsion) smears out the singularity. According to Hamer [38], regarding the low-lying levels as nearly degenerate, one can resort to the perturbation theory of the degenerated case and calculate the level-splitting (discontinuity of slope) explicitly. To be specific, we consider the matrix

$$V = \begin{pmatrix} V_{11} & V_{12} \\ V_{21} & V_{22} \end{pmatrix}, \quad (10)$$

with $V_{ij} = \langle i | \partial_K T | j \rangle$ and the transfer matrix T . The bases $|1\rangle$ and $|2\rangle$ are the (nearly degenerate) eigenvectors of T with the eigenvalues $\Lambda_{1,2}$, respectively. The states $\{|i\rangle\}$ are normalized so as to satisfy $\langle i | T | i \rangle = 1$. According to the perturbation theory, the eigenvalues of Eq. (10) yield the level-splitting slopes due to K . Hence, the latent heat (per unit cell) is given by a product of this discontinuity and the coupling constant $K(L)$,

$$Q(L) = |K(L)| \sqrt{(V_{11} - V_{22})^2 + 4V_{12}V_{21}} \frac{1}{2L}, \quad (11)$$

for the system size L .

In Fig. 4, we plot the latent heat Q (11) for $1/L^2$ and $6 \leq L \leq 14$. The least-squares fit for $L=6, 9, 12$ yields an estimate $Q=0.0482(59)$ in the thermodynamic limit $L \rightarrow \infty$.

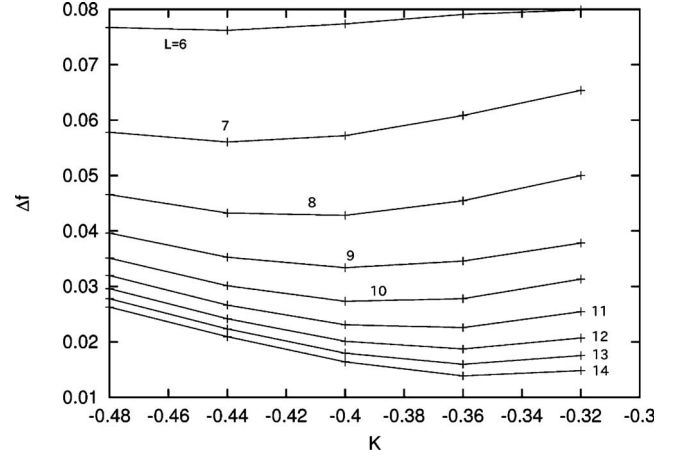


FIG. 5. The free-energy gap (7) is plotted for the bending rigidity K and the system sizes $6 \leq L \leq 14$. Tentatively, the defect parameter (5) is set to $K'=0$.

Similarly, for $L=1, 2 \bmod 3$, we obtain $Q=0.0391(38)$. Considering the deviation of these results as a possible systematic error, we obtain

$$Q = 0.043(10). \quad (12)$$

The error margin covers both the statistical and systematic errors.

We consider the $1/L^2$ -extrapolation scheme. The finite-size data are expected to converge rapidly (exponentially) to the thermodynamic limit around the first-order transition point for periodic boundary conditions, because the correlation length (typical length scale) ξ remains finite. Hence, the dominant finite-size corrections in our case should be described by $1/L^2$ (rather than $1/L$). On one hand, the curve in Fig. 4 appears to be concave down, indicating an existence of a correction of $O(1/L)$. However, this possibility (second-order phase transition) should be excluded: in a preliminary stage, we made a finite-size-scaling analysis and arrived at a conclusion that the scaling theory does not apply; the critical index ν estimated from the excitation gap tends to diverge as $L \rightarrow \infty$. Therefore, we set the abscissa scale in Fig. 4 to $1/L^2$; actually, the result in Fig. 3 demonstrates that the abscissa scale $1/L^2$ is sensible.

As a comparison, we provide a simulation result, setting the defect parameter to $K'=0$ tentatively. In Fig. 5, we present the free-energy gap Δf for the bending rigidity K ; the scale of K is the same as that of Fig. 2. Clearly, the data in Fig. 5 are less conclusive. As a matter of fact, the signatures of the crumpling transition strongly depend on the system size L . This result indicates that the choice of the defect parameter K' affects the finite-size behavior. In the preliminary stage, we survey a parameter space of K' and arrive at a conclusion that the above choice [Eq. (6)] is an optimal one.

In summary, the crumpling transition of the discrete planar folding in the $K < 0$ regime was investigated with the transfer-matrix method for $L \leq 14$. We adopted a modified folding rule (5), which enables us to implement the periodic-

boundary condition. As a result, we estimate the transition point and the latent heat as $K=-0.270(2)$ and $Q=0.043(10)$, respectively. The planar- and three-dimensional-folding models are closely related; see Eqs. (1) and (2). Making use of $K_3=-0.76(1)$ [33] and the present result $K=0.270(2)$, we arrive at $K_3/K=2.815(43)$ (~ 3). Relation (1) appears to hold satisfactorily; a slight deviation indicates that the truncation of the configuration space is not exactly validated. Encouraged by this result, we estimate $Q_3=0.043(10)$ via

Eq. (2). This result is consistent with $Q_3=0.03(2)$ [33] and $Q_3=0.05(5)$ [29], indicating that the singularity belongs to a weak-first-order transition rather definitely. Because a direct approach to the three-dimensional folding is computationally demanding, an indirect information from the planar folding would be valuable. A further justification of the configuration-space truncation would be desirable to confirm this claim. This problem will be addressed in the future study.

-
- [1] D. R. Nelson and L. Peliti, *J. Phys. (France)* **48**, 1085 (1987).
 [2] D. Nelson, T. Piran, and S. Weinberg, *Statistical Mechanics of Membranes and Surfaces*, Jerusalem Winter School for Theoretical Physics Vol. 5 (World Scientific, Singapore, 1989).
 [3] P. Ginsparg, F. David, and J. Zinn-Justin, *Fluctuating Geometries in Statistical Mechanics and Field Theory* (Elsevier Science, Amsterdam, 1996).
 [4] M. J. Bowick and A. Travesset, *Phys. Rep.* **344**, 255 (2001).
 [5] G. Gompper and D. M. Kroll, *J. Phys.: Condens. Matter* **9**, 8795 (1997).
 [6] Y. Kantor and D. R. Nelson, *Phys. Rev. Lett.* **58**, 2774 (1987).
 [7] Y. Kantor and D. R. Nelson, *Phys. Rev. A* **36**, 4020 (1987).
 [8] J.-P. Kownacki and D. Mouhanna, *Phys. Rev. E* **79**, 040101(R) (2009).
 [9] Y. Kantor, M. Kardar, and D. R. Nelson, *Phys. Rev. Lett.* **57**, 791 (1986).
 [10] Y. Kantor, M. Kardar, and D. R. Nelson, *Phys. Rev. A* **35**, 3056 (1987).
 [11] M. Baig, D. Espriu, and J. Wheeler, *Nucl. Phys. B* **314**, 587 (1989).
 [12] J. Ambjørn, B. Durhuus, and T. Jonsson, *Nucl. Phys. B* **316**, 526 (1989).
 [13] R. Renken and J. Kogut, *Nucl. Phys. B* **342**, 753 (1990).
 [14] R. Harnish and J. Wheeler, *Nucl. Phys. B* **350**, 861 (1991).
 [15] M. Baig, D. Espriu, and A. Travesset, *Nucl. Phys. B* **426**, 575 (1994).
 [16] M. Bowick, S. Catterall, M. Falcioni, G. Thorleifsson, and K. Anagnostopoulos, *J. Phys. I* **6**, 1321 (1996).
 [17] J. F. Wheeler and P. Stephenson, *Phys. Lett. B* **302**, 447 (1993).
 [18] J. F. Wheeler, *Nucl. Phys. B* **458**, 671 (1996).
 [19] F. David and E. Guitter, *EPL* **5**, 709 (1988).
 [20] P. Le Doussal and L. Radzihovsky, *Phys. Rev. Lett.* **69**, 1209 (1992).
 [21] D. Espriu and A. Travesset, *Nucl. Phys. B* **468**, 514 (1996).
 [22] M. Paczuski, M. Kardar, and D. R. Nelson, *Phys. Rev. Lett.* **60**, 2638 (1988).
 [23] J.-Ph. Kownacki and H. T. Diep, *Phys. Rev. E* **66**, 066105 (2002).
 [24] H. Koibuchi, N. Kusano, A. Nidaira, K. Suzuki, and M. Yamada, *Phys. Rev. E* **69**, 066139 (2004).
 [25] Y. Kantor and M. V. Jarić, *EPL* **11**, 157 (1990).
 [26] P. Di Francesco and E. Guitter, *EPL* **26**, 455 (1994).
 [27] P. Di Francesco and E. Guitter, *Phys. Rev. E* **50**, 4418 (1994).
 [28] E. N. M. Cirillo, G. Gonnella, and A. Pelizzola, *Phys. Rev. E* **53**, 1479 (1996).
 [29] Y. Nishiyama, *Phys. Rev. E* **81**, 041116 (2010).
 [30] M. Bowick, P. Di Francesco, O. Golinelli, and E. Guitter, *Nucl. Phys. B* **450**, 463 (1995).
 [31] E. N. M. Cirillo, G. Gonnella, and A. Pelizzola, *Phys. Rev. E* **53**, 3253 (1996).
 [32] M. Bowick, O. Golinelli, E. Guitter, and S. Mori, *Nucl. Phys. B* **495**, 583 (1997).
 [33] Y. Nishiyama, *Phys. Rev. E* **72**, 036104 (2005).
 [34] J. E. Moore and D. H. Lee, *Phys. Rev. B* **69**, 104511 (2004).
 [35] C. Castelnovo, C. Chamon, C. Mudry, and P. Pujol, *Phys. Rev. B* **72**, 104405 (2005).
 [36] P. Fendley, J. E. Moore, and C. Xu, *Phys. Rev. E* **75**, 051120 (2007).
 [37] R. L. Renken and J. B. Kogut, *Nucl. Phys. B* **350**, 554 (1991).
 [38] C. J. Hamer, *J. Phys. A* **16**, 3085 (1983).